Preliminary Development of a Multifunctional Hot Structure Heat Shield

Sandra P. Walker*, Kamran Daryabeigi†, Jamshid A. Samareh‡, and Sasan C. Armand §
NASA Langley Research Center, Hampton, Virginia, 23681

Scott V. Perino**
Crashworthiness for Aerospace Structures and Hybrids (CRASH) Lab
Virginia Tech, Blacksburg, Virginia, 24061

Development of a Multifunctional Hot Structure Heat Shield concept has initiated with the goal to provide advanced technology with significant benefits compared to the current state of the art heat shield technology. The concept is unique in integrating the function of the thermal protection system with the primary load carrying structural component. An advanced carbon-carbon material system has been evaluated for the load carrying structure, which will be utilized on the outer surface of the heat shield, and thus will operate as a hot structure exposed to the severe aerodynamic heating associated with planetary entry. Flexible, highly efficient blanket insulation has been sized for use underneath the hot structure to maintain desired internal temperatures. The approach was to develop a preliminary design to demonstrate feasibility of the concept. The preliminary results indicate that the concept has the potential to save both mass and volume with significantly less recession compared to traditional heat shield designs, and thus provide potential to enable new planetary missions.

I. Introduction

HEAT shields are a critical component on planetary entry vehicles. They provide the thermal protection needed on the windward surface for the vehicle to survive the severe aerodynamic heating environment which occurs when the vehicle traveling from space enters a planet's atmosphere. Traditional heat shield designs include the use of thermal protection system (TPS) materials on the outer most windward surface of the vehicle. Typically these TPS materials are designed to ablate and thus reduce heat transfer through the material to the underlying structure. The TPS materials are then bonded to a carrier structure.

The most recent state-of-the-art (SOA) heat shields have utilized materials designed to ablate. The Mars Science Laboratory (MSL) used Phenolic Impregnated Carbon Ablator (PICA), for the first time for Mars entry, as the heat shield TPS material.[1,2] Similarly, for returning to Earth from the International Space Station (ISS), SpaceX has been employing PICA-X on their Dragon spacecraft capsule heat shield.††

NASA has a great need for developing innovative entry vehicle decelerator systems for delivering higher payload masses to other planetary systems. Hypersonic Inflatable Aerodynamic Decelerator (HIAD) concepts are currently being developed at NASA. Flexible insulative TPS presently developed for HIADS is limited to a maximum entry heating rate of 44 to 66 Btu/ft^2/s (50 to 75 W/ cm^2), therefore requiring a large decelerator diameter of 33 to 49 ft (10 to 15 m); thus limiting its application to missions with low to medium entry velocities. Use of flexible ablative TPS concepts for HIADS, would potentially withstand heating rates up to 177 Btu/ft^2/s (200 W/cm^2) with corresponding shorter aerocapture/entry durations; and thus requiring a smaller decelerator diameter of 197 in (5 m).[3] Even though flexible ablative and insulative TPS HIAD concepts are very promising, they

* Assistant Branch Head and Research Aerospace Engineer, Structural Mechanics and Concepts Branch, MS 190.
† Research Aerospace Engineer, Structural Mechanics and Concepts Branch, MS 190, Senior Member.
‡ Aerospace Engineer, Vehicle Analysis Branch, MS 451, Associate Fellow.
§ Aerospace Engineer, Structural and Thermal Systems Branch, MS 431.
** LARSS, Structural Mechanics and Concepts Branch, MS 190, Student Member.
†† http://www.spacex.com/sites/spacex/files/pdf/DragonLabFactSheet.pdf [cited 18 November 2013]

may not be able to cover the entire design space needed for various planetary entry systems. Recently researchers have studied a hypersonic rigid deployable decelerator.[4]

This paper introduces a novel approach to a heat shield design. A multifunctional hot structure heat shield (MHSHS) concept is proposed for the purpose of providing a more efficient heat shield to enable future planetary missions. The MHSHS concept can be considered for a heat shield on a capsule with or without the additional use of rigid deployable decelerators depending on future mission requirements. A building block approach is being followed to develop the concept and thus assess feasibility. Consequently, this preliminary paper focuses on only the capsule heat shield, i.e., the heat shield without rigid deployable extensions. The work to develop the MHSHS concept is being funded at NASA Langley Research Center (LaRC) as an Internal Research and Development (IRAD) project.

An overview of the MHSHS concept is first introduced in the next section. The MHSHS is being directly compared here to a Baseline traditional heat shield in a preliminary trade study considering both structural and thermal performance for ISS return and Mars entry missions. The structural analysis effort included a heat shield applicable to ISS return. Finite element analysis is being utilized for the structural trade. Results of the structural analysis are then considered in the thermal analysis and preliminary thermal-structural sizing. Thermal sizing considered both ISS return heating and Mars entry heating load cases. Preliminary thermal testing is also presented. Results are compared between the MHSHS and Baseline concepts where feasibility and potential advantages of the MHSHS concept are identified. The status of the development effort is covered in this paper and future plans are discussed.

II. Concept Overview

The MHSHS concept is being pursued to offer advanced capability to enable future planetary missions. The concept is unique in integrating the TPS with the underlying carrier structure. Through integration of functions both mass and volume requirements within the spacecraft have the potential to be decreased. A ceramic matrix composite (CMC) material system will be employed for use as primary load carrying structure on the outer mold line (OML) of the heat shield (Fig. 1). Then flexible, super-lightweight blanket insulation can be sized underneath the CMC to achieve the desired inner mold line (IML) temperatures. This is a unique concept in having TPS material components also serve as primary load carrying structure, which offers the potential for overall weight savings in the aerospace vehicle design. This approach exploits the CMC material system capabilities. CMCs offer an attractive alternative to traditional TPS due to their ability to carry significant structural loads up to extreme temperatures approaching 3000°F (1649°C). Currently, CMCs have not been utilized in applications as primary load carrying structure on aerospace vehicles.

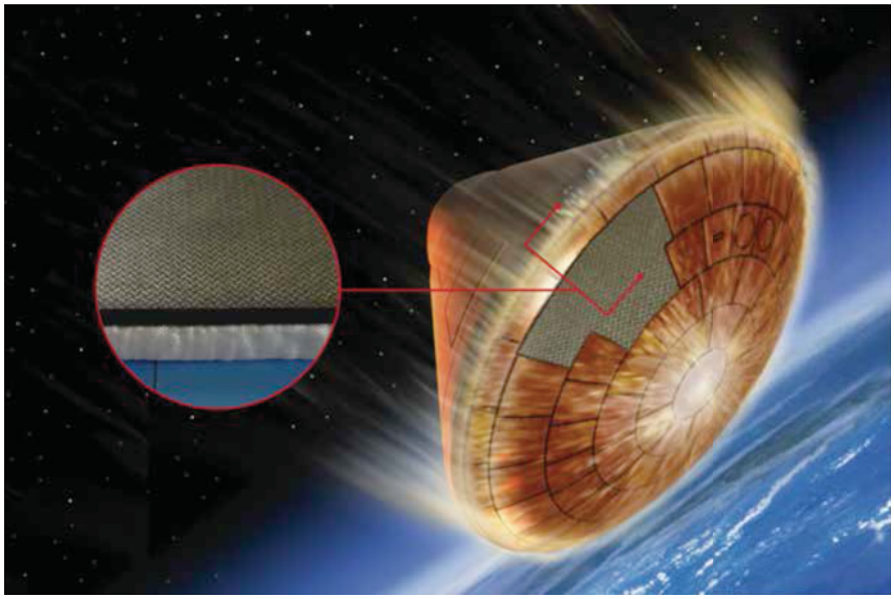

Figure 1. Illustration of Multifunctional Hot Structure Heat Shield concept and a close-up of carbon-carbon outer layer with blanket insulation underneath.

An advanced carbon-carbon (ACC-6) was the material chosen as the CMC outer layer to serve as the primary load carrying structure component of the heat shield.[5] ACC-6 was chosen due to the availability of a material property database and the cost. This material was under consideration in a Defense Advanced Research Projects Agency

(DARPA) program where the material property database was generated.[6] Although more advanced CMC's may be considered eventually which may offer additional structural capability and integrity, the availability of their material properties were limited, so the decision was made to initiate this work with the ACC-6 material system.

The current SOA in space vehicle heat shield technology separates the function of the TPS from the primary load carrying structure. This design approach is based on heritage TPS materials which traditionally are either ablative materials or ceramic tile insulation. Because these materials are extremely brittle, with very low load carrying capability, the design approach is currently to isolate the TPS from the structural loads. This has been accomplished by introducing a strain isolation pad (SIP) layer between the TPS and carrier structure. The layers in the traditional heat shield considered here as the Baseline are illustrated in Fig. 2a. PICA was chosen for the initial study as the current TPS material. As shown, the SIP layer is bonded to both the TPS material and carrier structure using room temperature vulcanizing (RTV) adhesive. The carrier structure shown is a titanium honeycomb sandwich construction being evaluated in this study.

Figure 2b illustrates the layers in the MHSHS concept being evaluated in this study. Here, the whole system is integrated in serving as the TPS. The ACC-6 outermost layer also serves as the primary load carrying structure. Shown in the figure is the ACC-6 skin. The concept being developed will also include additional frame T-stiffened structure, with the frames being composed of webs and flanges. The need for adhesive bonding the TPS to the structure is eliminated, thus eliminating bond line integrity and stress concentration issues, which can precipitate premature failures. Alternatively, other methods can be used to hold the insulation in place via the flanges to be considered. The super-lightweight blanket insulations being evaluated are discussed in a subsequent section.

The MHSHS concept can also be utilized as the heat shield in a rigid deployable system. The technology can be extended to include deployable extension components for missions requiring additional deceleration and thus may offer potential for more presision landing with greater stability in deployment compared to inflatable concepts. This preliminary study focuses on only the capsule heatshield.

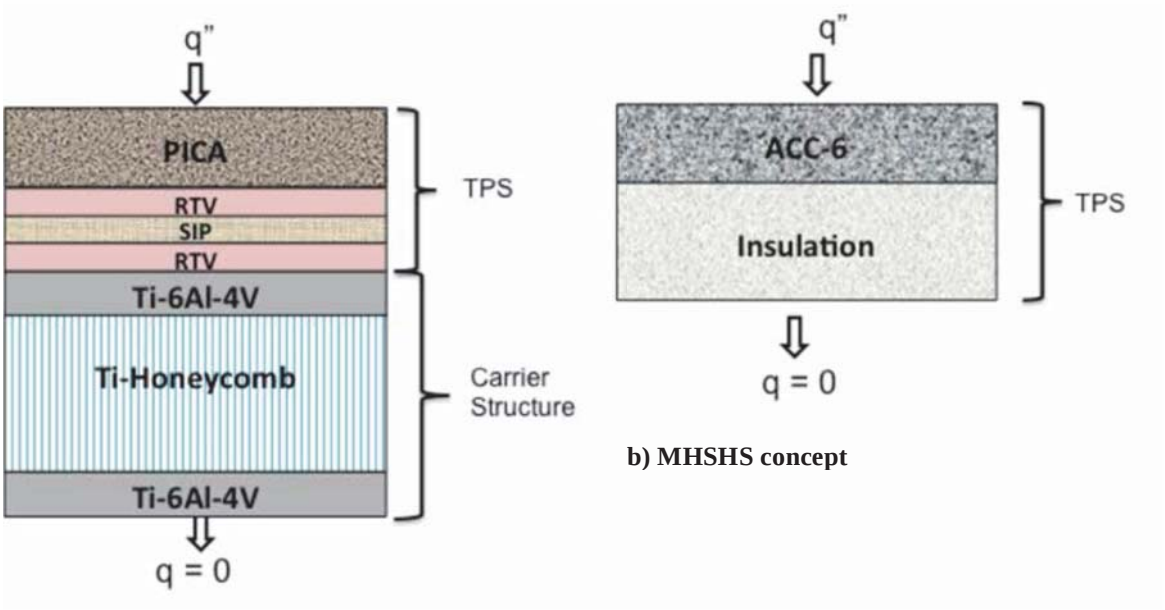

a) Baseline concept

b) MHSHS concept

Figure 2. Through-the-thickness layers of the a) Baseline and b) MHSHS concepts.

III. Structural Analysis and Results

The structural analysis effort is focused on a heat shield configuration that would be applicable to an ISS return mission spacecraft. A generic crew exploration vehicle (CEV) heat shield geometry was used in this preliminary trade study.[7] The finite element model (FEM) generated is displayed in Fig. 3. This heat shield has a 16-ft (4.9-m)

diameter and consists of a spherical center section surrounded by a shoulder region toroidal section. Also shown in Fig. 3 on the underside view are the locations of the structural constraints applied to the heat shield. There were 8 displacement constraints around the circumference shown by the magenta colored lines which represent where the heat shield would be attached to the frame skeleton of the crew module. Gaps were modeled at 16 locations, shown by the yellow colored lines, to constrain the heat shield from displacement under compression along where the crew module frame skeleton would be located.

Critical launch loads under consideration for performing the structural trade study include those loads that result from the severe vibro-acoustic launch environment. Due to the lack of existing vibro-acoustic data for the ACC-6 material system, data needed to be generated for the ACC-6 material system under consideration. Consequently, initial modal and acoustic testing has been conducted on ACC-6 panels and the data is being developed to generate vibro-acoustic loads associated with the Delta IV Heavy Launch vehicle. These loads will then be incorporated into the current structural analysis effort. Also, thermal stresses associated with entry need to be evaluated. This requires first the generation of the transient aero-heating distribution on the heat shield, which is planned in the project. Typically these stresses have not been as critical as other load cases. In the interim, the current structural sizing effort initiated by applying a 15 psi (1.034 x 10^5 Pa) pressure load to the spherical section of the heat shield. A factor of safety of 1.4 was applied to the maximum principal stress results and the distribution of the margin of safety is displayed in forthcoming contour plots. Quasi-static structural analysis was performed using MSC Nastran.[8]

The Baseline FEM consisted of modeling the titanium honeycomb sandwich structure with composite shell elements. For this study the facesheet thicknesses were held constant at 0.034-in (0.86 mm) and only the honeycomb core thickness was varied to obtain a baseline design with all positive margins of safety. A minimum core thickness of 3.25-in (82.6 mm) was determined adequate to provide the positive margins displayed in Fig. 4.

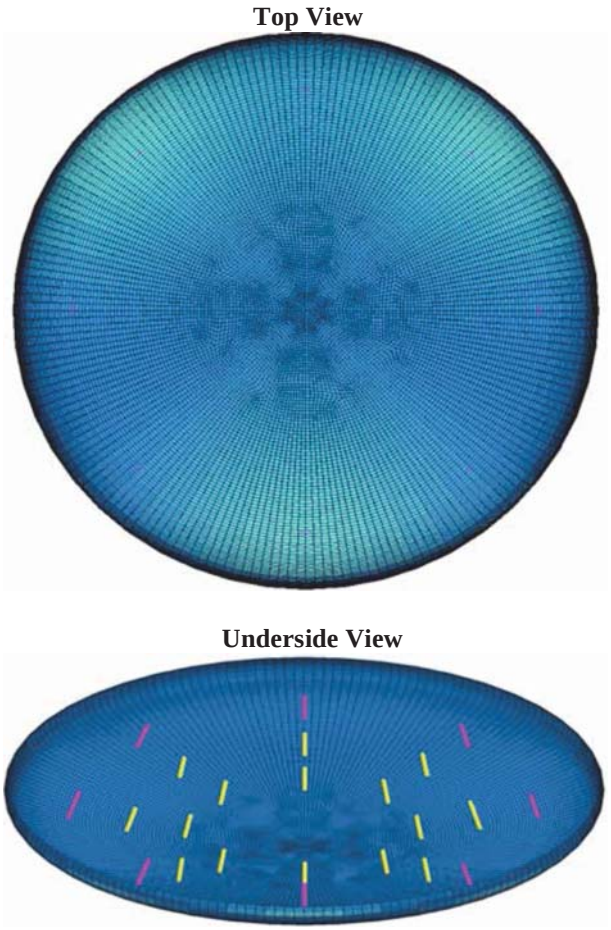

Figure 3. FEM of generic CEV heat shield.

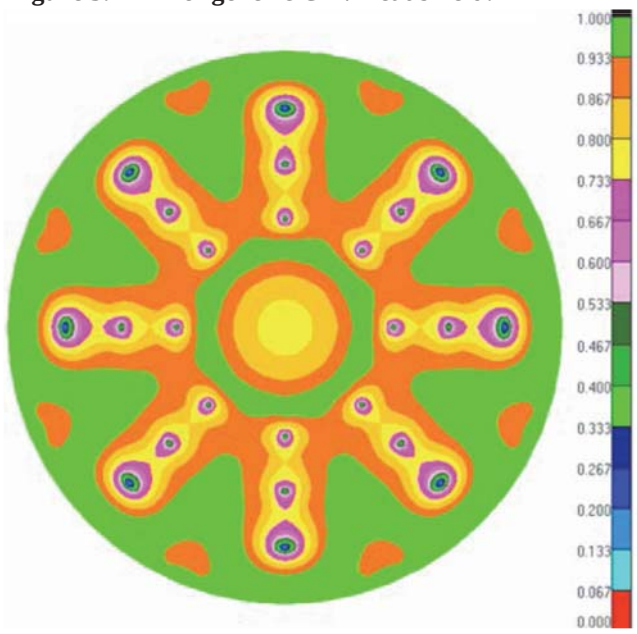

Figure 4. Baseline design margins of safety.

The MHSHS model consisted of modeling the ACC-6 skin as shell elements. Both a 0.25-in (6.35-mm) and a 0.5-in (12.7-mm) thick skin were considered. Since additional structure was needed, the 0.5-in (12.7-mm) thick skin was chosen for the concept and a mesh convergence study was performed. Beams were introduced to model T-stiffeners as displayed in Fig 5. The model contained three ring frames and eight radial stringers. The largest beam

Figure 5. MHSHS model showing the underside frame structure.

height in the model is 2-in (50.8 mm) total, which includes the height of the web and flange. Crossed beams were added across the displacement constraint points due to the large stress concentration predicted at the displacement constraints. These large stresses predicted need further investigation since each constraint should actually be distributed over an area in a more realistic model.

Positive margins were achievable with the addition of the crossed beams in this preliminary study using the point constraint. The margin distribution for the skin is displayed in Fig. 6. Shown in Fig. 7 are the margins for the maximum combined axial and bending stresses in the beams. The maximum stresses occurred on the outermost flange surface. Based on previous studies of frame stiffened structures, this very local outer flange surface stress has been determined to be over-predicted with finite element analyses[9], thus further investigation should be pursued with material bending tests of ACC-6.

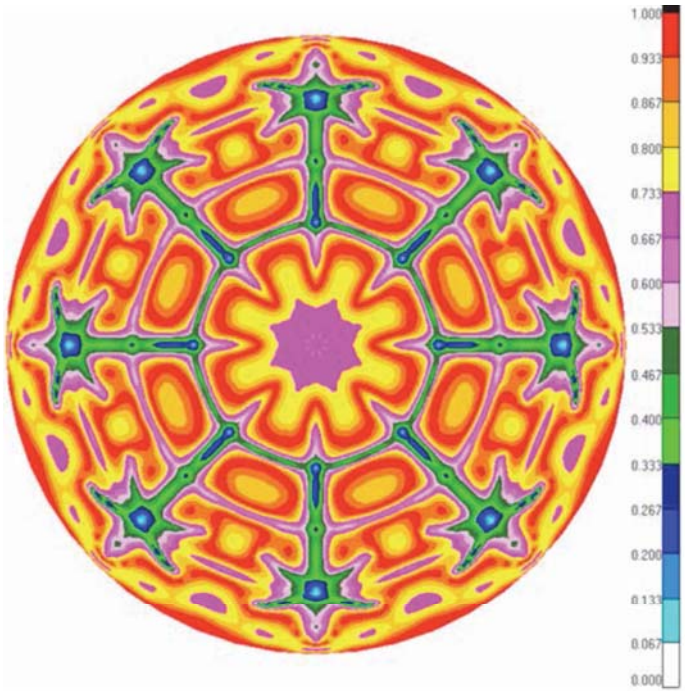

Figure 6. MHSHS model skin margins of safety.

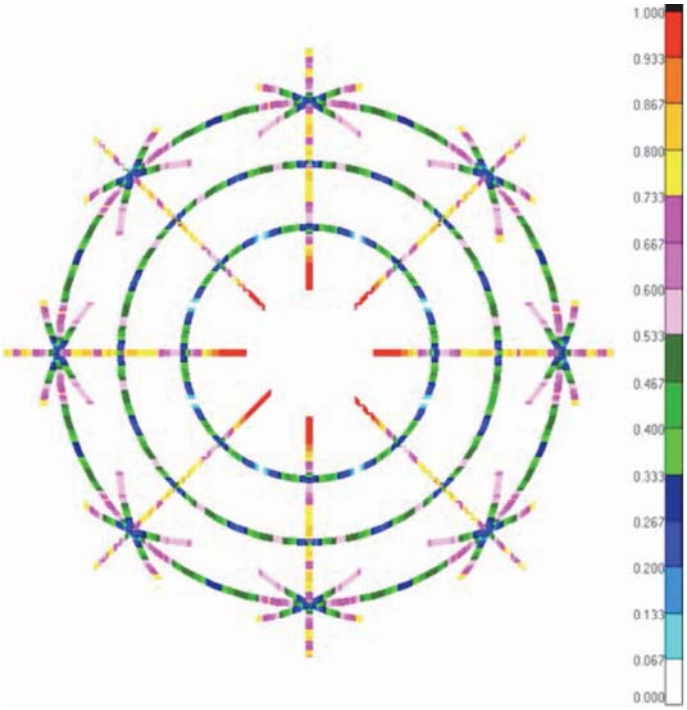

Figure 7. MHSHS model beam stiffener margins of safety.

IV. Aeroheating Environments

Aeroheating environments for a typical ISS return mission and a typical Mars entry mission are generated here for use as thermal loading conditions in the thermal analysis effort.

In this study, POST II was used to generate the ISS guided return trajectory. The POST II software[10] is a standard flight mechanics code that has been successfully used to solve a wide variety of atmospheric ascent and entry problems. The ISS return trajectory was generated for a 16.4 ft (5 m) vehicle with mass of 18,128 lb (8223 kg), entry velocity of 16777 mph (7.5 km/s) and lift to drag ratio (L/D) of 0.1. The trajectory velocity and density profiles were used to create the cold-wall heat flux profile using Sutton-Graves approximation.[11] The ratio of cold-wall heat flux over maximum cold-wall heat flux for ISS return is shown in Fig. 8. The TPS analysis was performed for maximum heat flux of 96.9 Btu/ft^2/s (110 W/cm^2). This profile was used to also perform parametric TPS analyses with maximum heating fluxes of 145.4 and 193.8 Btu/ft^2/s (165 and 220 W/cm^2).

The Mars entry heating profile is based on a preliminary MSL trajectory reconstruction.[12] This profile was used to create a cold-wall heating profile using Sutton-Graves approximation.[11] The Mars entry trajectory is generated for a 14.8 ft (4.5 m) diameter MSL vehicle with entry velocity of 13198 mph (5.9 km/s). The ratio of cold-wall heat flux over maximum cold-wall heat flux variation with time for Mars entry using Sutton-Graves approximation is also shown in Fig. 8. The cold-wall heating profile was scaled to perform parametric TPS analyses with maximum heating fluxes of 62 and 123 Btu/ft^2/s (70 and 140 W/cm^2). The Mars entry trajectory included jettisoning the heat shield prior to landing, similar to MSL entry.

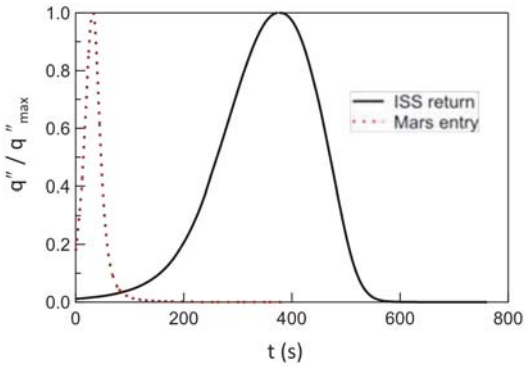

Figure 8. Estimated non-dimensional cold-wall heat flux variation for ISS return and Mars entry.

V. Thermal Analysis

The Fully Implicit Ablation and Thermal Response (FIAT) code[13] was used to perform thermal analysis and sizing of both the Baseline and MHSHS concept. Within FIAT material recession is also predicted in the ablating materials modeled. Thermal models for each concept are illustrated in Fig. 2. Note that this is a one-dimensional analysis so no structural frames were included in the thermal sizing study. The ISS return and Mars entry cold-wall heating profiles described in the previous section were used to create relevant environment profiles for input with FIAT. Both ISS and MSL estimated heating profiles were applied to each concept.

The material thermal properties for the various components were already included in the material database file supplied with FIAT for the Baseline model. FIAT was used to size the required thickness for PICA in the Baseline model for both ISS return and Mars entry using the parametric heating profiles. The thermal constraint in the model is the RTV temperature limit of 482°F (250°C). An adiabatic boundary condition was assumed for the bottom of the lower titanium facesheet.

The material thermal properties for the various components of the MHSHS model had to be integrated into the FIAT material database. The existing FIAT dimensionless mass blowing rate (B') tables for Reinforced Carbon-Carbon (RCC) were used for analyzing ACC-6. A multi-layer insulation approach was pursued considering several insulation materials. Opacified Fibrous Insulation (OFI) material was considered where thermal properties had been developed at NASA LaRC.[14] Alumina paper reinforced aluminosilicate aerogel was also included in the evaluation where material properties were obtained in the same test apparatus described in Ref. 14. The lower layer of the insulation consists of a thin layer 0.02 in (0.51 mm) of Nextel 440 fabric for holding the insulation in place. The fabric was modeled as a heat sink, with no heat loss from the backside, which is the standard conservative practice for TPS analysis. Parametric thermal studies were conducted with ACC-6 thicknesses of 0.25 and 0.50 in (6.35 and 12.7 mm) for the Mars entry case. For a single layer flexible insulation design, the OFI thickness was sized based on Nextel fabric IML temperature constraint of 302°F (150°C). Parametric studies were also conducted with IML temperature constraints varying between 392 and 572°F (200 to 300°C). As expected, insulation thickness and mass decreased with increasing IML temperature constraint. Only results with IML temperature constraint of 150°C are shown in this paper, and these results are the most conservative set of results. For a two-layer flexible insulation design, a 0.5 in (12.7 mm) thick layer of alumina paper reinforced aluminosilicate aerogel was used as the lower layer of insulation, and the OFI thickness was sized based on Nextel fabric IML temperature constraint of 302°F (150°C). OFI is efficient in reducing radiation which is the dominant mode of heat transfer at higher temperatures (closer to OML), while aerogels are effective in reducing gas conduction which is the dominant mode of heat transfer at lower temperatures (closer to IML) in high porosity insulations.[14]

VI. Thermal Testing

Preliminary testing has been initiated on coupon samples to validate the thermal models and demonstrate thermal performance. The Hypersonic Materials Environmental Test System (HYMETS) arc-jet facility at NASA LaRC (Fig. 9) was chosen for testing due to the ability to test small 1-in (25.4 mm) diameter specimens in an environment

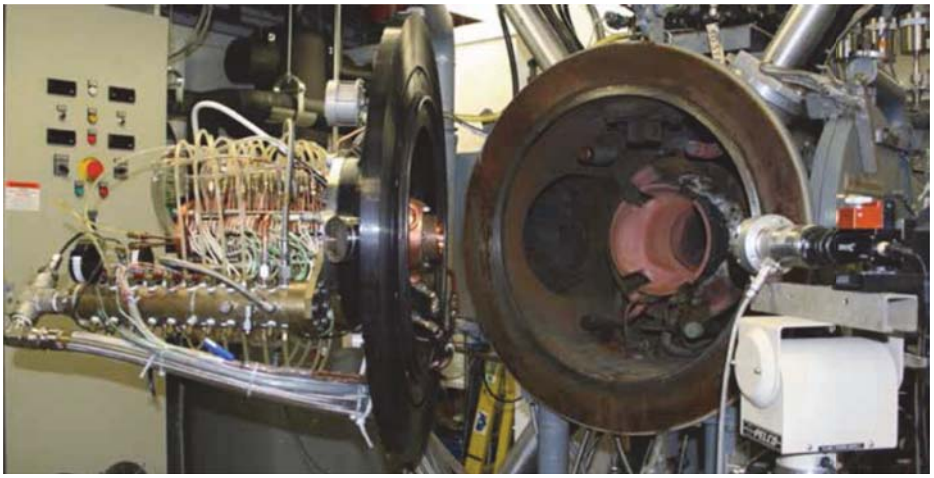

Figure 9. Photograph of HYMETS testing chamber opened for installing specimens.

simulating either Earth or Mars entry (Fig. 10).[15] Additional testing for both Earth and Martian entry conditions are being planned in the project.

A constant heating profile for a duration where the total integrated heat load matched that of the actual heating profile simulating ISS return was desired for this HYMETS test. The HYMETS heating profile generated is shown along with the ISS return heating profile in Fig. 11. For these profiles the actual ISS return integrated heat load is 21,300 Btu/ft^2 (242 x 10^6 J/m^2) where the HYMETS test integrated heat load is 19,800 Btu/ft^2 (225 x 10^6 J/m^2), which was considered to be adequate for these tests. Additionally, the facility was set to generate a test stagnation pressure of 0.036 atm (3648 Pa). The arc-jet testing was conducted on both PICA and ACC-6 specimens that were each 0.5-in (12.7 mm) thick.

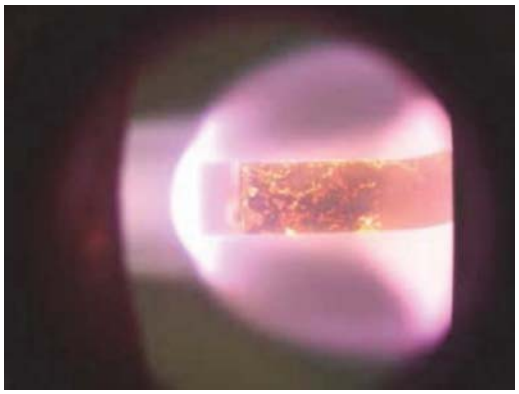

Figure 10. Photograph of specimen mounted on sting being test in HYMETS under Earth entry conditions.

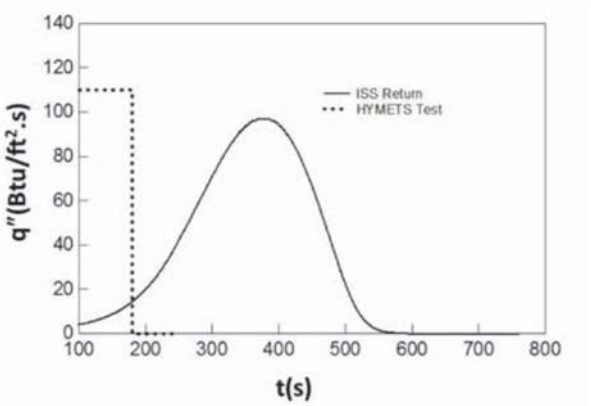

Figure 11. Heating profiles for HYMETS test and ISS return trajectory.

VII. Thermal Results and Discussion

Both thermal analysis and testing were conducted to perform thermal sizing and provide some preliminary data to evaluate feasibility. The thermal analysis focused on sizing both the Baseline and MHSHS concepts for both ISS return and Mars entry conditions. Arc-jet testing simulating the nominal ISS return heating profile was conducted to provide preliminary data to substantiate the FIAT analysis prediction, particularly the recession prediction, for both concepts.

The preliminary analysis results of the thermal sizing studies for ISS return are shown in Fig. 12 through 14, where both Baseline and MHSHS results are compared in each figure. For the Baseline design, the thickness of the PICA insulation is varied in the thermal sizing analysis. The static pressures at the end of the trajectory, especially at landing, are relatively high for ISS return; therefore, gas conduction is a significant mode of heat transfer for the MHSHS concept. Consequently, the insulation design for ISS return of the MHSHS concept consists of a double layer flexible insulation using 0.5 in (12.7 mm) thick of alumina paper reinforced aluminosilicate aerogel as the lower layer in the stack-up, with OFI as the upper layer. The OFI flexible insulation thickness is varied in the thermal analysis for each case subject to the IML temperature constraint of 302°F (150°C). The variation of the Baseline and MHSHS insulation thicknesses as a function of maximum cold-wall heat flux is shown in Fig. 12. The insulation thickness values shown have been normalized to the peak value predicted. The MHSHS flexible insulation thickness is less sensitive to the maximum cold wall heat fluxes compared to PICA. The resulting variation of overall heat shield system thickness with maximum cold-wall heat flux is provided in Fig 13.

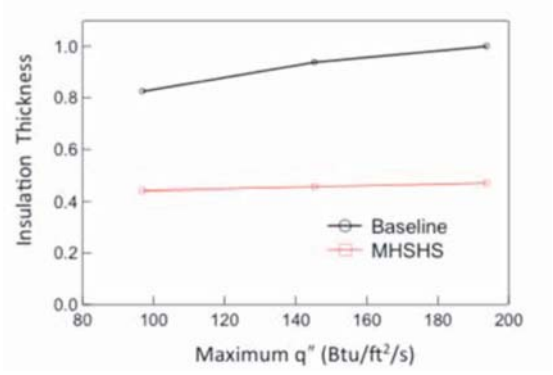

Figure 12. Normalized insulation thickness for Baseline and MHSHS concepts for various ISS return maximum cold-wall heat fluxes.

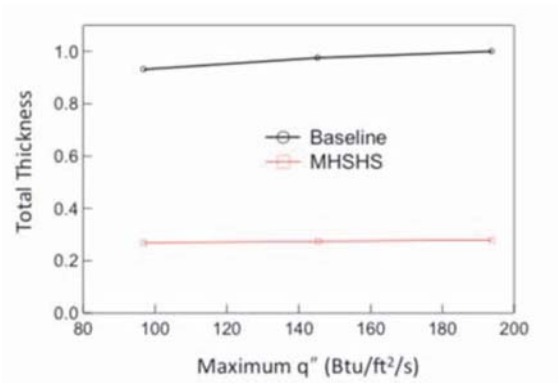

Figure 13. Normalized total heat shield thickness for Baseline and MHSHS concepts for various ISS return maximum cold-wall heat fluxes.

The total thickness value has been normalized to the peak predicted value. Based on these preliminary results the MHSHS would be more volumetrically efficient compared to the baseline concept. The preliminary estimates of variation of total recession with maximum heat fluxes for the Baseline and MHSHS concepts are shown in Fig. 14. The recession values have been normalized to the peak predicted value. MHSHS is observed to have significantly less recession than the Baseline concept and to be less sensitive to the variations in heat flux considered.

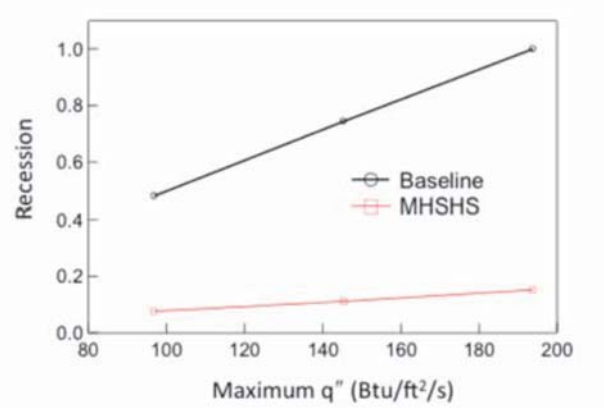

Figure 14. Normalized estimates of total recession for Baseline and MHSHS concepts for various ISS return maximum cold-wall heat fluxes.

The preliminary results of thermal sizing studies for Mars entry are shown in Fig. 15 through 17. In each figure, Baseline and MHSHS concept results are compared. The MHSHS studies were conducted with both ACC-6 thicknesses of 0.25 and 0.5 in (6.35 and 12.7 mm), since the structural design needs to be further developed for the Mars entry vehicle and structural load cases. For Mars entry, the static pressures throughout the trajectory are relatively low, and the heat shield is jettisoned before landing; therefore, gas conduction is not a significant mode of heat transfer for the MHSHS concept. Consequently, it was found that use of alumina paper reinforced aluminosilicate aerogel at the bottom of the insulation layers was not advantageous since aerogels are most effective for gas conduction.[14] Therefore, all the results presented here for Mars entry of MHSHS are for a single layer flexible insulation using OFI. The variation of required PICA thickness and flexible insulation thicknesses as a function of maximum cold-wall heat flux are shown in Fig. 15. The insulation thickness values shown have been normalized to the peak predicted value. The flexible insulation thickness is less sensitive to the maximum cold-wall heat flux compared to PICA. The required flexible insulation thickness is slightly higher for the thinner ACC-6, as expected. The preliminary estimates of variation of total recession with maximum heat flux for the Baseline and MHSHS concept are shown in Fig. 16. The recession values shown have been normalized to the peal predicted value. The AAC-6 is predicted to have significantly less recession than the Baseline concept and also to be less sensitive to the variations in heat flux considered. The variation of resulting maximum wall temperature with

maximum heat flux for the Baseline and MHSHS concepts are shown in Fig. 17. The maximum wall temperatures values shown have been normalized to the peak predicted value. The predicted temperatures for ACC-6 are slightly lower compared to PICA, with the 0.50 in (12.7 mm) thick ACC-6 having lower maximum wall temperatures compared to the 0.25 in (6.35 mm) thick ACC-6.

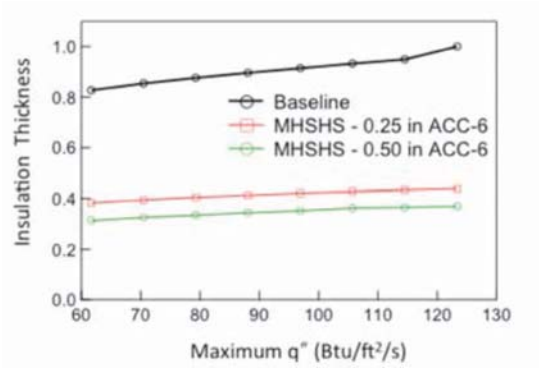

Figure 15. Normalized insulation thickness for Baseline and MHSHS concepts for various Mars entry maximum cold-wall heat fluxes.

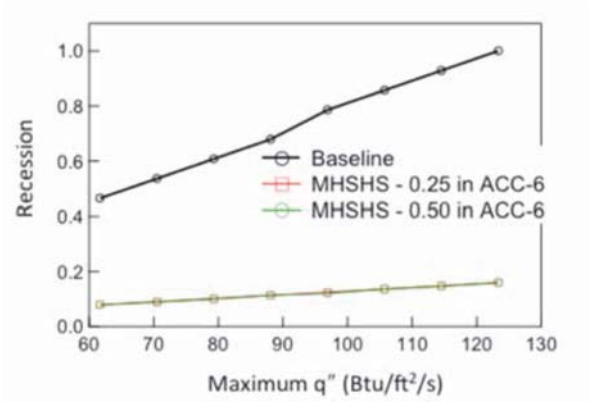

Figure 16. Normalized estimates of total recession for Baseline and MHSHS concepts for various Mars entry maximum cold-wall heat fluxes.

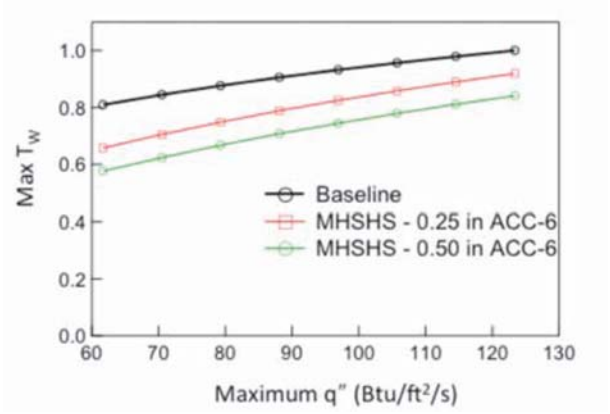

Figure 17. Normalized maximum surface temperature predictions for Baseline TPS and MHSHS concepts for various Mars entry maximum cold-wall heat fluxes.

The HYMETS arc-jet testing was conducted on the samples shown in Figure 18. A photograph prior to testing is given in Fig. 18a along with the backside insulation (white disc) used in the tests. A photograph after testing in the

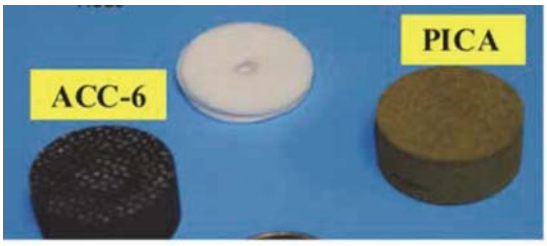

a) Pre-test specimens

b) Post-test specimens

Figure 18. Photographs of pre- and post –test specimens.

nominal ISS return simulated environment is given in Fig. 18b along with a quarter to indicate size. As can be observed from the photographs, significant recession occurred for the PICA sample. Pre- and post-test measurements taken are given in Table 1. Due to the very brittle nature of the charred post-test PICA specimen, a thickness measurement could not be made. However, a mass loss of 55% was measured for PICA compared to a mass loss of less than 10% for the ACC-6 specimen. The ACC-6 specimen receded 0.06 in (1.52 mm), which was less than the predicted recession. This may be due to either the slightly lower total integrated heat load for the HYMETS test condition or conservative approximations used in the FIAT code. However, these results substantiate the thermal models as being adequate for predicting recession. The results also demonstrate the ability of the ACC-6 material system to withstand the severe ISS return heating with minimal recession, compared to PICA.

Table 1. HYMETS test results

	Mass oz (g)		**%Mass Loss**	**Thickness in (mm)**		**Recession in (mm)**
	Pre-test	Post-test		Pre-test	Post-test	
PICA	0.067 (1.90)	0.030 (0.85)	55	0.5 (12.7)	NA	NA
ACC-6	0.338 (9.58)	0.306 (8.67)	9.7	0.5 (12.7)	0.44 (11.2)	0.06 (1.52)

VIII. Preliminary Integrated Thermal-Structural Design Evaluation

For the nominal ISS return trajectory, results from the structural evaluation were incorporated in the one-dimensional thermal model. The scope of the current structural evaluation included a 15 psi load case applied to a generic CEV heat shield configuration. The integrated thermal-structural design results, although preliminary, are evidence of the potential of the MHSHS concept. Heat shield thickness results from Fig. 12 and 13 are shown again in Table 2 along with the added frame height determined from the structural evaluation. The values shown here have been normalized to the peak total thickness value. Together, the integrated thermal-structural results show a significant increase in volumetric efficiency for the MHSHS concept compared to the Baseline, traditional heat shield design. Heat shield mass results are compared in Table 3. Preliminary results indict mass saving may be feasible for the MHSHS concept. Note that the masses predicted here have not been optimized. Thus, structural optimization could lead to additional mass savings for the MHSHS concept.

Table 2. Preliminary ISS return mission normalized heat shield thickness results

	Baseline	**MHSHS concept**
External TPS	0.37	none
Structure	0.63	0.10
Internal Insulation	none	0.19
Additional Frame Height	none	0.19
TOTAL	1.0	0.48

Based on these preliminary results, the MHSHS concept appears to be a feasible alternative to the Baseline, traditional heat shield design. The MHSHS concept has the potential to save both mass and volume for a heat shield design while offering other potential benefits including less recession and lower risk in eliminating the adhesive bonding of the TPS to carrier structure.

Table 3. Preliminary ISS return mission mass results

	Baseline lb (kg)	MHSHS concept lb (kg)
External TPS	1132 (513)	none
Structure	657 (298)	1413 (641)
Internal Insulation	none	225 (102)
TOTAL	1789 (811)	1638 (743)

IX. Concluding Remarks

Development of a Multifunctional Hot Structure Heat Shield concept has been initiated. Preliminary results demonstrate feasibility. The concept could provide an alternative to traditional heat shields on planetary entry vehicles. The new concept has the potential to save both weight and volume while offering other benefits including less recession and lower risk. Consequently, further evaluation is recommended to mature the concept using a building block approach. Coupon testing needs to continue and include Mars entry arc-jet testing and critical material behavior tests. More refined load cases need to be developed and investigated with higher fidelity thermal-structural analyses. Subcomponent testing under critical thermal-structural loads should follow. After subcomponent configurations are defined, vehicle integration will need to be addressed with joining concepts being evaluated. An ISS return mission could then be identified to demonstrate the technology for future use on a Mars mission. As future Mars mission requirements become better defined, the potential exists to offer an alternative heat shield concept including a rigid deployable system that may be enabling to future Mars missions.

Acknowledgments

The authors would like to acknowledge W. Keith Belvin, Chief Technologist, Martin Waszak, Deputy Chief Technologist, and members of the Langley Technology Council (LTC) for providing the funding, support, and oversight for this IRAD project.

References

[1]Edquist, Karl T., Dyakonov, Artem A., Wright, Michael J. and Tang, Chun Y., “Aerothermodynamic Design of the Mars Science Laboratory Heatshield,” AIAA Paper 2009-4075, AIAA Thermophysics Conference, San Antonio, Texas, 2009.

[2]Wright, M., Beck, R., Edquist, K., Driver, D., Sepka, S., and Slimko, E., “Sizing and Margins Assessment of the Mars Science Laboratory Aeroshell Thermal Protection System," AIAA Paper 2009-4231, AIAA Thermophysics Conference, San Antonio, Texas, June 2009.

[3]Zang, T.A. et al., “Overview of the NASA Entry, Descent and Landing Systems Analysis Study,” AIAA–2010–8649, 2010.

[4]Cruz-Ayoroa, et al., “Mass Model Development for Conceptual Design of a Hypersonic Rigid Deployable Decelerator,” International Planetary Probe Workshop, Toulouse, France, 2012.

[5]Thompson, J. , “Final Report, 3000°F Carbon-Carbon Materials for Falcon Leading Edges,” Carbon-Carbon Advanced Technologies, Inc., Fort Worth, TX, March 2006.

[6]Glass, D. E., Dirling, R., Croop, H., Fry, T. J., and Frank, G. J., “ Materials for Hypersonic Flight Vehicles,” AIAA-2006-8122, AIAA/AHI International Space Planes And Hypersonic Systems And Technologies Conference, Volume 3, Canberra, Australia, November 2006.

[7]Owens, D. B., Aubuchon, V. V., “Overview of Orion Crew Module and Launch Abort Vehicle Dynamic Stability,” AIAA Paper 2011-3504, AIAA Applied Aerodynamics Conference, Honolulu, HI, June 2011.

[8]MSC Nastran 2012.2 Quick Reference Guide, MSC Software Corporation, Santa Ana, CA, 2012.

[9] Przekop, A., Wu, H. T., Shaw, P., “Nonlinear Finite Element Analysis of a Composite Non-Cylindrical Pressurized Aircraft Fuselage Structure”, AIAA SciTech Conference, January 2014 (submitted for publication).

[10]G. L. Brauer et al.: Program To Optimize Simulated Trajectories (POST): Volume 1, Formulation Manual. Martin Marietta Corporation, 1990.

[11] Sutton, K., and Graves, R. A., Jr., " A general Stagnation-Point Convective-Heating Equation For Arbitrary Gas Mixtures," NASA Technical Report R-376, November 1971.

[12] Bose, D., White, T., Santos, J. A., Feldman, J., Mahzari, M., Olson, M, and Laub, B., "Initial Assessment of Mars Science Laboratory Heatshield Instrumentation and Flight Data," AIAA Paper 2013-0908, January 2013.

[13] Chen, Y. K., Milos, F. S., "Ablation and Thermal Response Program for Spacecraft Heatshield Analysis," Journal of Spacecraft and Rockets, Vol. 36, No. 3, May-June 1999, pp.475-483.

[14] Daryabeigi, K., Cunnington, G. R., Miller, S. D., and Knutson, J. R., "Combined Heat Transfer in High-Porosity High-Temperature Fibrous Insulations: Theory and Experimental Validation," AIAA Paper 2010-4660, June 2010.

[15] Splinter, S. C., Bey, K. S., Gragg, J. G., " Comparative Measurements of Earth and Martian Entry Environments in the NASA Langley HYMETS Facility," AIAA-2011-1014, Aerospace Sciences Meetings, January, 2011.